Special Issue Article

Advances in Mechanical Engineering

Advances in Mechanical Engineering
2017, Vol. 9(3) 1–11

DOI: 10.1177/1687814017696415
journals.sagepub.com/home/ade
SAGE

Flood fragility analysis for bridges with multiple failure modes

Hyunjun Kim[1], Sung-Han Sim[1], Jaebeom Lee[1], Young-Joo Lee[1] and Jin-Man Kim[2]

Abstract

Bridges are one of the most important infrastructure systems that provide public and economic bases for humankind. It is also widely known that bridges are exposed to a variety of flood-related risk factors such as bridge scour, structural deterioration, and debris accumulation, which can cause structural damage and even failure of bridges through a variety of failure modes. However, flood fragility has not received as much attention as seismic fragility despite the significant amount of damage and costs resulting from flood hazards. There have been few research efforts to estimate the flood fragility of bridges considering various flood-related factors and the corresponding failure modes. Therefore, this study proposes a new approach for bridge flood fragility analysis. To obtain accurate flood fragility estimates, reliability analysis is performed in conjunction with finite element analysis, which can sophisticatedly simulate the structural response of a bridge under a flood by accounting for flood-related risk factors. The proposed approach is applied to a numerical example of an actual bridge in Korea. Flood fragility curves accounting for multiple failure modes, including lack of pier ductility or pile ductility, pier rebar rupture, pile rupture, and deck loss, are derived and presented in this study.

Keywords

Bridge, flood fragility, reliability analysis, finite element analysis, multiple failure modes

Date received: 20 September 2016; accepted: 7 February 2017

Academic Editor: Yonghui An

Introduction

With the recent unprecedented growth of the global economy and rapid technological advances in civil engineering, a number of bridges have been constructed to build transportation systems that provide public and economic bases for humankind. However, it is also widely known that bridges are exposed to risks from natural hazards such as floods, earthquakes, and typhoons. These diverse hazards often cause structural damage to bridges, even resulting in their collapse. Because a bridge failure can cause huge casualties, economic losses, and social problems, an accurate assessment of the structural vulnerability of bridges to natural hazards is critical to effective design and maintenance of bridges.

Defined as the relationship between hazard intensity and the probability that a bridge is damaged more than to a certain level, bridge fragility curves have been widely used to express the structural vulnerability of a bridge subjects to a variety of natural hazards. However, previous studies have mainly focused on the fragility curve derivation for bridges under earthquakes. For example, Basoz et al.[1] and Shinozuka et al.[2] developed empirical fragility curves using a data set of bridge damages resulting from the 1994

[1]School of Urban and Environmental Engineering, Ulsan National Institute of Science and Technology (UNIST), Ulsan, Republic of Korea
[2]Geotechnical Engineering Research Institute, Korea Institute of Construction Technology (KICT), Goyang-Si, Republic of Korea

Corresponding author:
Young-Joo Lee, School of Urban and Environmental Engineering, Ulsan National Institute of Science and Technology (UNIST), 50 UNIST-gil, Ulsan 44919, Republic of Korea.
Email: ylee@unist.ac.kr

Northridge earthquake and the 1995 Kobe earthquake, respectively. Alternatively, Karim and Yamazaki[3] generated analytical fragility curves of the highway bridge piers utilizing a numerical simulation based on the 1995 Kobe earthquake data. Choi et al.[4] modeled a type of bridge built in the central and southeastern United States to produce analytical fragility curves for identifying vulnerabilities under an earthquake. In addition, Yang et al.[5] presented the analytical fragility curves of six bridge types such as multi-span simply supported concrete and steel bridges, multi-span continuous concrete and steel bridges, and single-span concrete and steel bridges. Seo et al.[6] proposed a method for fragility curve derivation considering unknown truck characteristics, to quantify the structural integrity of in-service highway bridges. In these studies, a wide variety of seismic fragility curves of bridges were obtained either empirically or analytically, and the results were used to assess the structural integrity of bridges under earthquakes.

In comparison with seismic fragility analysis, fragility analysis related to floods has received less attention. Decò and Frangopol[7] generated the fragility curves of highway bridges under multiple hazards including earthquake, scour, traffic load, and environmental attack. With a similar approach, Dong et al.[8] derived seismic fragility curves of bridges considering the effects of scour and corrosion. In addition, Dawson et al.[9] assessed the flood risk vulnerability of a fluvial dike system, and Witzany and Cejka[10] performed a numerical analysis of flood fragility of a stone vault bridge structure. However, these studies mainly focused on the derivation of seismic fragility curves, while flood-related risk factors such as scour and corrosion were considered as an alternative cause of bridge failure in addition to earthquakes. As such, there have been few studies on the flood fragility estimation of bridges.

However, various flood-related factors such as water stream pressure, debris accumulation, corrosion, and scour are reported as the most common causes of bridge failure.[11,12] In reality, a flood often generates a rapid water flow with accumulated debris, which yields a combined loading impact on bridges via the service loads and may bring about structural damage or collapse. Furthermore, if the structural integrity of a bridge is significantly degraded by the corrosion of steel reinforcements in addition to the scour-induced removal of soil resistances, the failure risk of bridges under flood events increases and their failure modes can become more complex.

Recently, Lee et al.[13] proposed to perform reliability analysis in conjunction with finite element analysis (i.e. finite element reliability analysis) to derive flood fragility curves of bridges. However, this research focused on the suggestion of a computational platform for performing finite element reliability analysis, and only some of the flood-related factors and bridge failure modes were addressed. In the research, the water pressure increase due to debris accumulation and structural deterioration caused by corrosion were considered in the finite element model of a target bridge, and only the lack of ductility of the bridge pier was introduced as a failure mode. While this work presented a fundamental methodology for flood fragility analysis, flood-related factors and bridge failure modes were found to be limited. In reality, scour is also an important risk factor during a flood, and bridges may collapse with more diverse failure modes than only lack of ductility. To obtain more realistic and accurate fragility curves of bridges against floods, these flood-related factors and failure modes should be carefully addressed in the fragility analysis.

In this study, a new approach for flood fragility analysis is developed to evaluate the structural vulnerability of bridges under floods. Bridge scour around piers is simulated in a finite element model using the flood-related factors discussed in Lee et al.[13] In addition, various bridge failure modes, including the lack of pier ductility, the lack of pile ductility, pier rebar rupture, pile rupture, and deck loss, are considered during the flood fragility analysis. The proposed approach is then applied to a numerical example of an actual bridge in Korea.

Proposed approach for flood fragility analysis

To conduct a proper analysis for flood fragility curve derivation, the proposed approach suggests simulating flood-related factors, such as bridge scour, in a finite element model. Additionally, it is necessary to consider the critical failure modes of bridges subject to floods. Furthermore, to perform finite element reliability analysis and calculate the probability of bridge failure efficiently, a Python-based interface for FERUM and ABAQUS (PIFA)[13] is introduced as a computational platform.

Flood-related factors in consideration

To evaluate bridge fragility under floods accurately, as previously mentioned, essential flood-related factors that can cause damages to bridges need to be included in the flood fragility analysis. This study considers the following critical flood-related factors to conduct a more realistic flood fragility analysis: (1) bridge scour, (2) structural deterioration of steel reinforcements and piles due to corrosion, and (3) the increased water pressure due to debris accumulation around bride piers. These three factors account for more than 50% of bridge failures according to a survey study on causes of

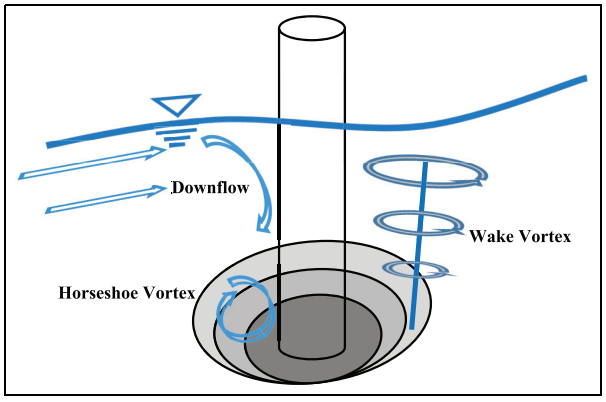

Figure 1. Occurrence of the scour hole during a flood.

bridge failure in the United States between 1987 and 2011.[12]

Bridge scour. Bridge scour is known as one of the most common causes of bridge failure during a flood. When a flood occurs, the water velocity rapidly increases from upstream to downstream, bringing the downflow water from the water surface to the bottom around the bridge piers, as shown in Figure 1. The downflow water primarily produces a scour hole by removing the sediments from the vicinity of the foundations. The horseshoe vortex and wake vortex are subsequently generated from the dissimilar flow depths, which create a scour hole to a certain depth. Such bridge scour can occur at all of the bridge foundations, and the depth depends on various factors such as water velocity, pier dimensions, and sediment types. Because bridge scour directly affects the stability of a whole bridge system, reasonable consideration of the scour in a finite element model is important for realistic flood fragility analysis.

Bridge scour is taken into account in the finite element modeling by employing adjustable scour depths for each bridge pier. To simplify the finite element model, the soil can be modeled with horizontal rigid elements that are attached to bridge piers or piles to provide fixed boundary conditions. When a part of the soil is removed due to bridge scour, the stiffness values of the corresponding rigid elements are set to a negligibly small value to eliminate stiffness provided by the elements to the structure.

The scour depth for a single pier can be determined by an empirical equation[14] defined as

$$S = 1.564 \times \chi^{0.405} \times \left(\frac{v}{\sqrt{g \times d}}\right)^{0.413} \quad (1)$$

where S is the scour depth, χ is the relative approach flow depth, v is the water velocity, g is the gravitational acceleration, and d is the depth of the approach flow. The calculated scour depth is used to select the rigid elements corresponding to the removed soil; thus, stiffness needs to be set to a small value to simulate the scour. However, the stiffness values of the springs below the calculated scour depth remain unchanged from the originally fixed condition.

As a bridge typically has multiple piles, the scour depths around each pile vary depending on their geometric shapes, locations, and arrangement. Various studies have been conducted to estimate the scour hole depth experimentally[15–17] with different sets of conditions including pile arrangement, water velocity, spacing, and sediment size. It was observed in these studies that the ratio of scour hole depths at the first three piles with respect to the first pile was nearly 1:0.94:0.90, despite different values of sediment particle size, water velocity, and pile spacing. Because studies on the scour depths at piles extending beyond the third are few, the scour depth calculated by equation (1) and a scour depth ratio of 1:0.94:0.90 are used in the finite element model of this study.

Structural deterioration of steel reinforcements and piles due to corrosion. Another primary flood-related factor of bridge failure is structural deterioration resulting from the corrosion of steel reinforcements and piles. When water infiltrates into the concrete and subsequently contacts with a steel reinforcement, the stiffness of a bridge can be significantly diminished as the effective area reduces. Thoft-Christensen et al.[18] considered the reduction of the cross-sectional area of steel reinforcements based on the following time-dependent model

$$A(t) = \begin{cases} D_i^2 \frac{\pi}{4} & \text{for } t \le T_i \\ [D(t)]^2 \frac{\pi}{4} & \text{for } T_i < t < T_i + \frac{D_i}{r_{corr}} \\ 0 & \text{for } t \ge T_i + \frac{D_i}{r_{corr}} \end{cases} \quad (2)$$

where $A(t)$ is the effective cross-sectional area of steel reinforcement, D_i is the diameter of steel reinforcements, T_i is the corrosion onset time, r_{corr} is the rate of corrosion reflecting both the thickness of the concrete cover and the water–cement ration, and $D(t)$ is the effective diameter of steel reinforcements following a lapse of t years. In addition, the effective diameter $D(t)$ can be calculated using the following equation

$$D(t) = D_i - r_{corr} \times (t - T_i) \quad (3)$$

The corrosion of bridge piles is also considered in this study based on the work of Decker et al.[19] When the bridge piles are exposed to high chloride concentration, the average corrosion rate is 13 μm/year, which has been experimentally proven.[18] This corrosion rate is introduced to describe the corrosion of steel reinforcement and piles during a flood in this study.

Table 1. Drag coefficient.

Pier type	C_D
Semicircular-nosed pier	0.7
Square-ended pier	1.4
Debris lodged against the pier	1.4
Wedged-nosed pier with nose angle 90° or less	0.8

Increased water pressure due to debris accumulation. Finally, a high level of water velocity is generally observed during a flood, but debris accumulation that often happens around bridge piers may lead to increase in water velocity level. Regarding the water velocity increase, American Association of State Highway and Transportation Officials (AASHTO)[20] and Korean Highway Bridge Design Specification (KHBDS) suggest the following equation for estimating water pressure (P_w) considering the impact of accumulated debris[21]

$$p_w = 5.14 \times 10^{-4} \times C_D \times v^2 \tag{4}$$

where v is the water velocity and C_D is the drag coefficient which can be determined from pier type, as shown in Table 1. It is noteworthy in Table 1 that the drag coefficient gets the maximum value (i.e. 1.4) with lodged debris. The calculated water pressure is then applied to bridge piers as an external load.

The collision force from the floating debris can cause bridge failure. However, this loading effect is excluded in this study because it was observed from a preliminary analysis that the collision force due to debris such as wood yields a negligible impact as compared with other flood-related factors such as scour, structural deterioration, and water pressure and debris. Furthermore, AASHTO[20] and KHBDS[21] no longer suggest considering the collision force in their recent guidelines of bridge design.

Bridge failure modes and hazard intensity measure

When a bridge is exposed to a heavy flood, the flood-related factors described in section "Flood-related factors in consideration" can result in failure of the bridge with several different failure modes. As aforementioned, a fragility curve illustrates the relationship between a hazard intensity and the exceedance probability with a failure mode. For example, a peak ground acceleration (PGA) is generally used as the intensity measure for seismic fragility curves. In other words, a fragility curve quantifies the likelihood of experiencing a certain level of structural damage with a given failure mode defined by structural responses such as excessive stress or displacement.[22] Similarly, failure modes and an intensity measure need to be defined for the derivation of fragility curves against floods, but it is a challenging task because there are several different failure modes and flood intensity–related factors. In this study, three different types of failure modes are considered as follows: (1) lack of displacement ductility, (2) steel rupture, and (3) deck loss.

Lack of displacement ductility. First, the displacement ductility demand (M_D) is defined according to the ratio of the imposed post-elastic deformation, which is mathematically defined by the following equation[23]

$$M_D = \frac{\Delta_D}{\Delta_{Y(i)}} \tag{5}$$

where Δ_D is the maximum displacement of a structural member and $\Delta_{Y(i)}$ is the displacement at the yielding point of the member. The displacement ductility is calculated at both bridge piers and piles in this study in order to check the ductile failure of bridges.

Steel rupture. In addition, steel rupture is defined as the case of maximum stress at steel reinforcements or bridge piles reaching ultimate stress, which is defined by the following equation

$$\sigma_{max} > \sigma_u \tag{6}$$

where σ_u is the ultimate stress and σ_{max} is the maximum stress at steel reinforcements or bridge piles.

Deck loss. Deck loss is assumed to occur when the deck displacement is greater than a certain value resulting in the deck dislodging from the bridge bearing. This is expressed in the following equation

$$\Delta_{Pier} - \Delta_{Deck} > \Delta_{Bearing} \tag{7}$$

where $\Delta_{Bearing}$ is the bearing length, and Δ_{Pier} and Δ_{Deck} are the maximum displacements of the pier and deck, respectively. When the relative displacement between pier and deck is greater than the length of the bridge bearing, the bridge is evaluated as having a brittle failure.

The water velocity is selected as the intensity measure of the flood fragility curve. In bridge design, one of the critical water loads is stream pressure. AASHTO[20] defines this water pressure as the pressure of flowing water acting in the longitudinal direction of bridge substructures, such as piers. Floating debris accumulates around piers and decks, resulting in increased water pressure on the bridge and frequent overflow that may induce secondary flood damage. Regarding the effect of piled debris on the water force, AASHTO[20] also suggests a function of mean flow velocity. In that sense, the water velocity is introduced as a reasonable intensity

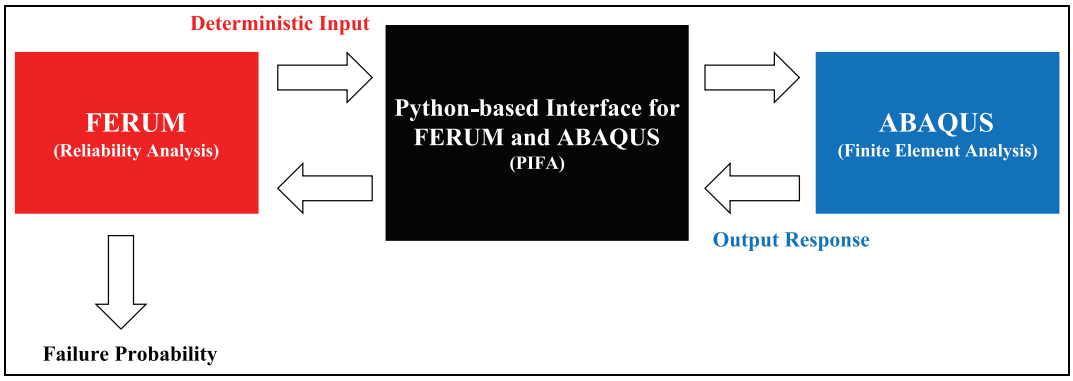

Figure 2. Schematic flow of the software platform.

measure to determine bridge failure in this study. Whereas the water level may also be an appropriate intensity measure, it is introduced as a deterministic parameter at its maximum value (i.e. the pier height) because we assume that a bridge is in a heavy flood and the water level reaches the maximum.

Software platform for calculating probability of failures

For increased accuracy in the analysis of bridge flood fragility, the flood-related factors and failure modes described in sections "Flood-related factors in consideration" and "Bridge failure modes and hazard intensity measure" need to be sophisticatedly modeled for structural analysis using methods such as finite element analysis. A fragility curve is generally obtained from structural reliability analysis that requires repeated structural analyses. Consideration of the flood-related factors and failure modes in a finite element model can render each finite element analysis computationally expensive, subsequently increasing the time cost of flood fragility curve derivation.

To overcome this challenge and calculate the probability of bridge failure in an accurate and efficient manner, a PIFA, which was recently developed as a computational platform for finite element reliability analysis in Lee et al.,[13] is employed in this research. As shown in Figure 2, this computational platform consists of three components: (1) finite element reliability using MATLAB (FERUM) for reliability analysis, (2) ABAQUS for finite element analysis, and (3) a python-based interface for connecting these two software packages. FERUM[24] is an open-source software package built in MATLAB, developed by researchers at the University of California, Berkeley to conduct reliability analysis using various methodologies including first-order reliability method (FORM).[25] ABAQUS is a widely used commercial software package for finite element analysis.

In the platform, PIFA was carefully designed to control the overall process of finite element reliability analysis efficiently through interaction with FERUM and ABAQUS. As shown in Figure 2, FERUM repeatedly provides deterministic input values of random variables for PIFA so that it can automatically construct finite element models with varying input values and deliver them to ABAQUS. Then, ABAQUS performs finite element analyses and returns the desired structural output responses (e.g. stress and displacement), which are then sent to FERUM via PIFA. Based on the structural responses, FERUM performs reliability analysis employing FORM, which is a widely used method of reliability analysis. More details on the computational platform and FORM can be found in Lee et al.[13] and Der Kiureghian,[25] respectively.

Example application of the proposed approach

As an application example, the proposed approach of flood fragility analysis is applied to a real bridge in Korea. The name of the bridge used in this example is the Wangsukcheon Bridge that was reported to have collapsed in 2001 due to bridge scour around piers. A simple design drawing of the collapsed bridge was obtained from a regional department, but unfortunately, more detailed information could not be found. In addition, a new bridge was built in the same location following the collapse and is now in service. Thus, a finite element model of the bridge is constructed based on the acquired design drawing of the bridge, but designs of other similar bridges of that time are also considered. The constructed model is subsequently used in flood fragility analysis employing the proposed approach.

Finite element model

To derive flood fragility curves using the proposed methodology, a finite element model of the

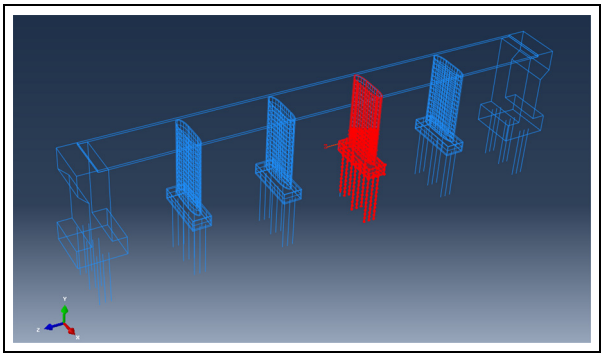

Figure 3. Finite element model of the Wangsukcheon Bridge.

Table 2. Properties of the Wangsukcheon Bridge.

Total length (m)	50.4
Height of piers (m)	8.1
Width of piers (m)	5
Length of piles (m)	6

Wangsukcheon Bridge is built using ABAQUS, as shown in Figure 3. The finite element model consists of reinforced concrete piers and steel piles. According to the design drawing of the target bridge, piers are connected to a deck using isolated bearings, allowing individual consideration of each pier. Therefore, only one pier located at the bridge center (red pier in Figure 3) is considered in the finite element model shown in Figure 4, in order to save on time cost of fragility curve derivation. In the finite element model, the interactions between concrete and steel reinforcements of the pier are represented by embedded elements of ABAQUS. More detailed information on the example bridge is presented in Table 2.

To simulate the removal of soil resistances at the bridge piles due to the occurrence of scour holes, the bridge piles are equally spaced and modeled with horizontal springs, as shown in Figure 4. With a given water velocity, the scour hole depth is calculated using equation (1), and the stiffness values of the springs installed above the depth are changed to zero, which describes the removal of soil resistance down to the scour depth. In addition, the ratio of scour hole depth described in section "Flood-related factors in consideration" is applied to determine the scour depth behind the first pile.

The material nonlinearity of concrete and steel is also considered in the model to simulate the structural response realistically. Among the diverse models to simulate this nonlinear behavior, the strain–stress curves obtained from Le Roux and Wium[26] and Shima and Tamai[27] are used in this study, considering the concrete and steel used in the target bridge. Selected strain–stress curves are presented in Figure 5.

Statistical parameters and limit-states

Using appropriate statistical properties of random variables is a key to accurate fragility estimates. In this research, two kinds of uncertainties are considered and assumed as random variables: mass and water pressure intensity; the statistical properties of these random variables are shown in Table 3. As shown in Table 3, a total of four random variables are introduced in this example, and all random variables are assumed to be independent. These statistical properties were carefully introduced based on the works of Lehký et al.,[28] Ju et al.,[29] and Kolisko et al.[30] following an extensive literature review. It is also noteworthy that the water pressure intensity is multiplied by the water pressure as

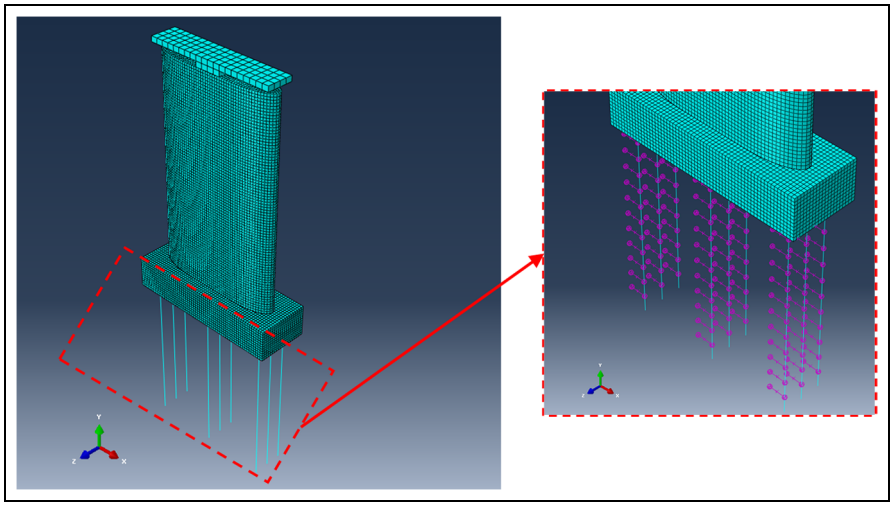

Figure 4. Finite element model of the bridge pier.

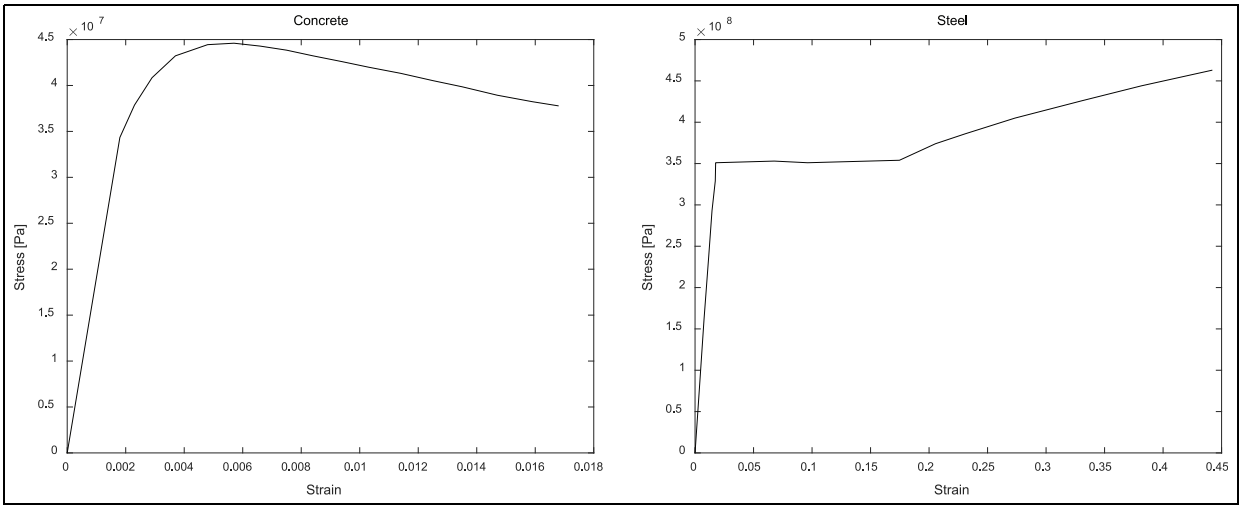

Figure 5. Strain–stress curves of concrete (left) and steel (right).

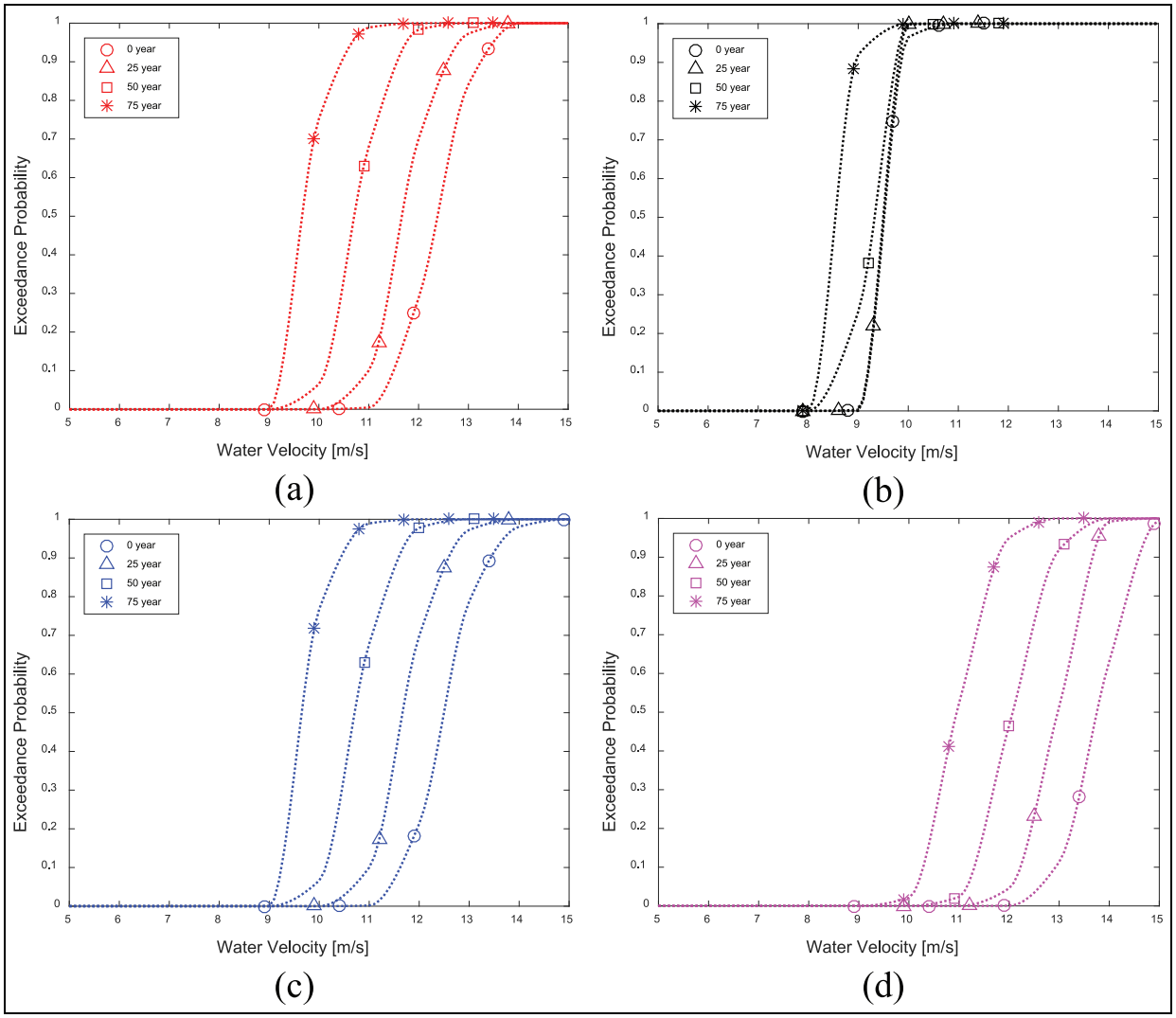

Figure 6. Flood fragility curves for various periods of structural deterioration with (a) deck loss, (b) first plastic hinge occurrence, (c) second plastic hinge occurrence, and (d) collapse.

Table 3. Statistical properties of random variables.

	Mean	Standard deviation	Coefficient of variation	Distribution type
Concrete mass density	2300 kg/m^3	115 kg/m^3	0.05	Normal
Steel bar mass density	7861.5 kg/m^3	314.5 kg/m^3	0.04	Normal
Pile steel mass density	7868.6 kg/m^3	314.7 kg/m^3	0.04	Normal
Water pressure intensity	1	0.1	0.10	Normal

Table 4. Damage states and corresponding ductility demands.

Damage state	Ductility demand
Minor damage (first plastic hinge occurrence)	$1 \leqslant M_D \leqslant 3.3$
Major damage (second plastic hinge occurrence)	$3.3 \leqslant M_D \leqslant 7.0$
Collapse	$M_D > 7.0$

calculated from equation (4) to consider the uncertainty of water velocity.

In a fragility analysis, limit-states are defined to deal with different failure modes of bridges. As mentioned in section "Bridge failure modes and hazard intensity measure," the following kinds of failure modes are considered in this example: (1) lack of displacement ductility, (2) steel rupture, and (3) deck loss. Since the first two

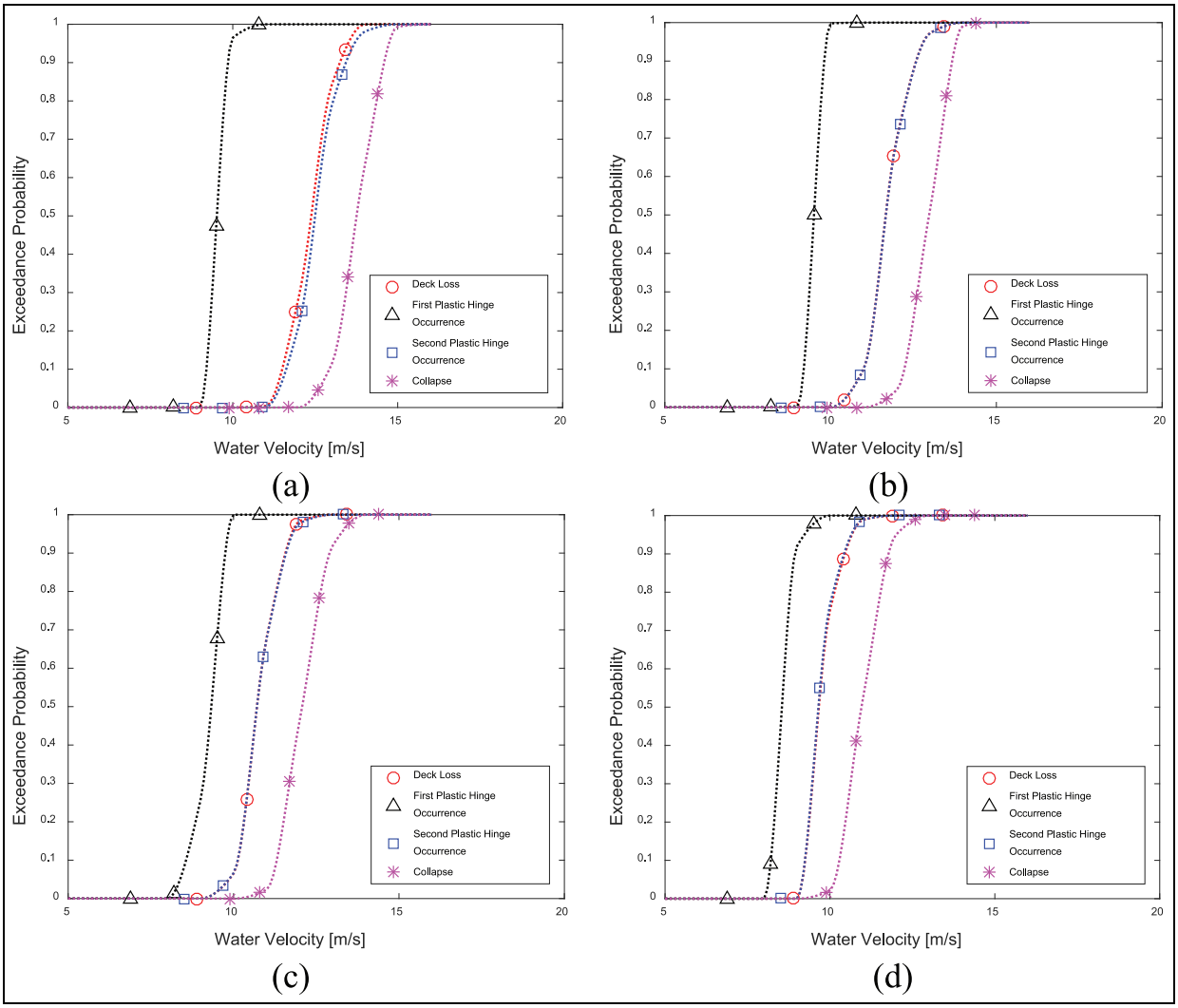

Figure 7. Flood fragility curves with various damage states succeeding structural deterioration for (a) 0 year, (b) 25 years, (c) 50 years, and (d) 75 years.

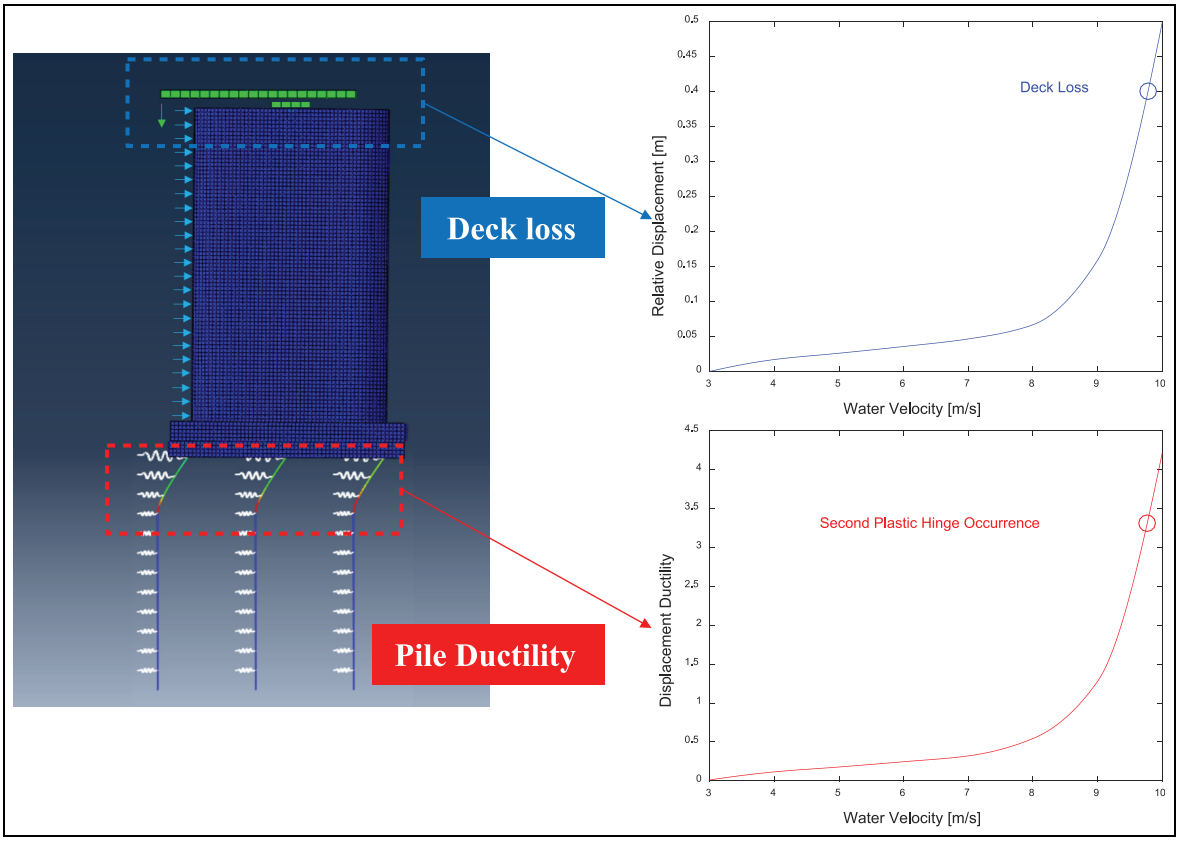

Figure 8. The analysis results of deck loss and second plastic hinge occurrence.

criteria can be applied to both piers and piles, a total of five limit-states are assumed in this example: the lack of pier ductility, lack of pile ductility, pier rebar rupture, pile rupture, and deck loss.

The limit-states of displacement ductility are defined as the three damage states (i.e. minor damage, major damage, and collapse), as shown in Table 4, which is introduced from the works of Song et al.[31] and Chiou et al.[32] The three damage states are defined by ductility demand (M_D), which can be calculated by equation (5), and the structural meanings of the first two damage states are the first and second occurrences of plastic hinge, respectively. Note that when the second plastic hinge occurs, the displacement is rapidly increased due to the external load. In addition, the criteria for steel rupture and deck loss are considered as 0.436 GPa of the ultimate strength and 0.4 m of the bearing length, respectively.

Analysis result: flood fragility curves

Employing the proposed approach, fragility analysis of the example bridge against floods is conducted, and the corresponding analysis results are shown in Figures 6 and 7. Initially, the performance of fragility analysis with all five of the limit-states described in section "Statistical parameters and limit-states" was attempted, but the results showed that three of the failure modes (i.e. lack of pier ductility, pier rebar rupture, and pile rupture) occur when the water velocity exceeds 20 m/s. Considering water velocity during an extreme flood ranges from 3 to 10 m/s,[33,34] risk of these three failure modes is seen to be negligible, thus Figures 6 and 7 show only the fragility curves for the remaining two failure modes (i.e. lack of pile ductility and deck loss).

The fragility estimates of all limit-states increase with aging of the bridge. To display this more clearly, the fragility curve of each limit-state at different deterioration periods is plotted in Figure 6. From Figure 6, it is observed that structural deterioration of steel reinforcement due to corrosion can give a significant impact on flood fragility estimates because the effective area of steel reinforcement decreases with time.

Flood fragility curves with several deterioration periods are subsequently illustrated in Figure 7. The fragility curves in Figure 7 detail four damage states (i.e. first plastic hinge occurrence, second plastic hinge occurrence, collapse, and deck loss) succeeding 0, 25, 50, and 75 years of structural deterioration, respectively. As presumed, 0-year deterioration represents the intact bridge. As shown in the curves, the exceedance probability generally increases with increasing water velocity because a large water velocity means a deep scour hole and strong water pressure, as expressed in equations (1)

and (4), respectively. It is also noteworthy that the order of the occurrence likelihood of structural damages is as follows: first plastic hinge occurrence, deck loss, second plastic hinge occurrence, and collapse.

In addition, the fragility results in Figure 7 show that deck loss and the occurrence of the second plastic hinge take place at nearly the same water velocity, which represents the deck displacement suddenly increasing due to the occurrence of the second plastic hinge at bridge piles. To verify this phenomenon, a deterministic finite element analysis is conducted with various water velocities, employing the mean values of random variables; the analysis results are shown in Figure 8. As shown in Figure 8, when the water velocity exceeds approximately 9 m/s, the relative displacement between pier and deck, and the displacement ductility of piles, reaches their corresponding failures of deck loss and second plastic hinge occurrence at nearly equivalent water velocities.

Conclusion

This study developed a new approach for deriving flood fragility curves of bridges subject to floods with multiple failure modes. For accurate flood fragility estimates, it was suggested to consider bridge scour, structural deterioration due to corrosion, and water velocity increase due to debris accumulation in the construction of a bridge finite element model. However, this can make fragility analysis that is based on finite element reliability analysis computationally expensive, so it was also suggested to use a PIFA as a computational platform for the analysis. The proposed approach was applied to an actual bridge in Korea, and the analysis results revealed that the flood fragilities increased with increasing water velocity. In addition, it was observed that the occurrence likelihood of structural damages was in the following order: first hinge occurrence, deck loss and second plastic hinge occurrence, and collapse. The analysis results also showed that the exceedance probabilities of damage states increased with the increasing period of structural deterioration. These findings confirm the successful application of the proposed approach to the derivation of flood fragility curves of bridges.

Declaration of conflicting interests

The author(s) declared no potential conflicts of interest with respect to the research, authorship, and/or publication of this article.

Funding

The author(s) disclosed receipt of the following financial support for the research, authorship, and/or publication of this article: This research was supported by a grant (16SCIP-B065985-04) from Smart Civil Infrastructure Research Program funded by Ministry of Land, Infrastructure and Transport (MOLIT) of Korea Government and Korea Agency for Infrastructure Technology Advancement (KAIA).

References

1. Basoz NI, Kiremidjian AS, King SA, et al. Statistical analysis of bridge damage data from the 1994 Northridge, CA, earthquake. *Earthq Spectra* 1999; 15: 25–54.
2. Shinozuka M, Feng MQ, Lee J, et al. Statistical analysis of fragility curves. *J Eng Mech* 2000; 126: 1224–1231.
3. Karim KR and Yamazaki F. Effect of earthquake ground motions on fragility curves of highway bridge piers based on numerical simulation. *Earthq Eng Struct D* 2001; 30: 1839–1856.
4. Choi E, DesRoches R and Nielson B. Seismic fragility of typical bridges in moderate seismic zones. *Eng Struct* 2004; 26: 187–199.
5. Yang CSW, Wemer SD and DesRoches R. Seismic fragility analysis of skewed bridges in the central southeastern United States. *Eng Struct* 2015; 83: 116–128.
6. Seo J, Hatfield G and Kimn JH. Probabilistic structural integrity evaluation of a highway steel bridge under unknown trucks. *J Struct Int Maint* 2016; 1: 65–72.
7. Decò A and Frangopol DM. Risk assessment of highway bridges under multiple hazards. *J Risk Res* 2011; 14: 1057–1089.
8. Dong Y, Frangopol DM and Saydam D. Time-variant sustainability assessment of seismically vulnerable bridges subjected to multiple hazards. *Earthq Eng Struct D* 2013; 42: 1451–1467.
9. Dawson R, Hall J, Sayers P, et al. Sampling-based flood risk analysis for fluvial dike systems. *Stoch Env Res Risk A* 2005; 19: 388–402.
10. Witzany J and Cejka T. Reliability and failure resistance of the stone bridge structure of Charles Bridge during floods. *J Civ Eng Manag* 2007; 13: 227–236.
11. Wardhana K and Hadipriono FC. Analysis of recent bridge failures in the United States. *J Perform Constr Fac* 2003; 17: 144–150.
12. Cook W. *Bridge failure rates, consequences, and predictive trends*. PhD Thesis, Utah State University, Logan, UT, 2014.
13. Lee J, Lee YJ, Kim H, et al. A new methodology development for flood fragility curve derivation considering structural deterioration for bridges. *Smart Struct Syst* 2016; 17: 149–165.
14. Yanmaz AM. Uncertainty of local scouring parameters around bridge piers. *Turkish J Engin Environ Sci* 2001; 25: 127–137.
15. Ataie-Ashtiani B and Beheshti AA. Experimental investigation of clear-water local scour at pile groups. *J Hydraul Eng* 2006; 132: 1100–1104.
16. Heidarpour M, Afzalimehr H and Izadinia E. Reduction of local scour around bridge pier groups using collars. *Int J Sediment Res* 2010; 25: 411–422.
17. Akib S, Jahangirzadeh A and Basser H. Local scour around complex pier groups and combined piles at semi-integral bridge. *J Hydrol Hydromech* 2014; 62: 108–116.

18. Thoft-Christensen P, Jensen FM, Middleton CR, et al. *Revised rules for concrete bridges*. London: Thomas Telford Ltd., 1997.
19. Decker JB, Rollins KM and Ellsworth JC. Corrosion rate evaluation and prediction for piles based on long-term field performance. *J Geotech Geoenviron* 2008; 134: 341–351.
20. American Association of State Highway and Transportation Officials (AASHTO). *AASHTO LRFD bridge design specifications*. 6th ed. Washington, DC: AASHTO, 2000.
21. Korea Road & Transportation Association (KRTA). *Korean Highway Bridge Design Specification (KHBDS)*. Seoul, Korea: KRTA, 2010.
22. Lee Y-J and Moon D-S. A new methodology of the development of seismic fragility curves. *Smart Struct Syst* 2014; 14: 847–867.
23. Caltrans. *Seismic design criteria*. Sacramento, CA: California DOT, 2006.
24. Haukaas T. *Finite element reliability and sensitivity methods for performance-based engineering*. PhD Thesis, University of California, Berkeley, CA, 2003.
25. Der Kiureghian A. *First- and second-order reliability methods*. Boca Raton, FL: CRC Press, 2005.
26. Le Roux RC and Wium JA. Assessment of the behaviour factor for the seismic design of reinforced concrete structural walls according to SANS 10160—part 4: technical paper. *J S Afr Inst Civ Eng* 2012; 54: 69–80.
27. Shima H and Tamai S. Tension stiffness model under reversed loading including post yield range. *IABSE Colloq* 1987; 54: 547–556.
28. Lehký D, Keršner Z and Novák D. Determination of statistical material parameters of concrete using fracture test and inverse analysis based on FraMePID-3PB tool. In: *Proceedings of the 5th international conference on reliable engineering computing*, Brno, 13–15 June 2012. Czech Republic: LITERA, pp.261–270.
29. Ju M, Oh H and Sun JW. Simplified reliability estimation for optimum strengthening ratio of 30-year-old double T-beam railway bridge by NSM techniques. *Math Probl Eng* 2014; 734016: 1–10.
30. Kolisko J, Hunka P and Jung K. A statistical analysis of the modulus of elasticity and compressive strength of concrete C45/55 for pre-stressed precast beams. *J Civil Eng Architect* 2012; 6: 1571–1576.
31. Song ST, Chai YH and Hale TH. Limit state analysis of fixed-head concrete piles under lateral loads. In: *Proceedings of the 13th world conference on earthquake engineering*, Vancouver, BC, Canada, 1–6 August 2004, pp.1–15.
32. Chiou JS, Chiang CH, Yang HH, et al. Developing fragility curves for a pile-supported wharf. *Soil Dyn Earthq Eng* 2011; 31: 830–840.
33. Terry K. Flood and related debris flow hazards, Las Vegas SE quadrangle, Nevada. Report, University of Nevada-Reno, Reno, NV, 1986.
34. City of Alexandria Virginia. Lake Barcroft Inundation study extracted data for City of Alexandria, https://www.alexandriava.gov/LakeBarcroftDam (accessed 7 February 2017).